JACS
JOURNAL OF THE AMERICAN CHEMICAL SOCIETY
Article
pubs.acs.org/JACS

The Mechanism of Substrate Inhibition in Human Indoleamine 2,3-Dioxygenase

Igor Efimov,[†] Jaswir Basran,[‡] Xiao Sun,[†] Nishma Chauhan,[†] Stephen K. Chapman,[§] Christopher G. Mowat,[⊥] and Emma Lloyd Raven*[,†]

[†]Department of Chemistry, University of Leicester, University Road, Leicester LE1 7RH, United Kingdom
[‡]Department of Biochemistry, University of Leicester, Lancaster Road, Leicester LE1 9HN, United Kingdom
[§]Heriot-Watt University, George Heriot Wing, Edinburgh EH14 4AS, United Kingdom
[⊥]EaStCHEM, School of Chemistry, University of Edinburgh, West Mains Road, Edinburgh EH9 3JJ, United Kingdom

Supporting Information

ABSTRACT: Indoleamine 2,3-dioxygenase catalyzes the O_2-dependent oxidation of L-tryptophan (L-Trp) to *N*-formylkynurenine (NFK) as part of the kynurenine pathway. Inhibition of enzyme activity at high L-Trp concentrations was first noted more than 30 years ago, but the mechanism of inhibition has not been established. Using a combination of kinetic and reduction potential measurements, we present evidence showing that inhibition of enzyme activity in human indoleamine 2,3-dioxygenase (hIDO) and a number of site-directed variants during turnover with L-tryptophan (L-Trp) can be accounted for by the sequential, ordered binding of O_2 and L-Trp. Analysis of the data shows that at low concentrations of L-Trp, O_2 binds first followed by the binding of L-Trp; at higher concentrations of L-Trp, the order of binding is reversed. In addition, we show that the heme reduction potential (E_m^0) has a regulatory role in controlling the overall rate of catalysis (and hence the extent of inhibition) because there is a quantifiable correlation between E_m^0 (that increases in the presence of L-Trp) and the rate constant for O_2 binding. This means that the initial formation of ferric superoxide ($Fe^{3+}-O_2^{\bullet-}$) from Fe^{2+}-O_2 becomes thermodynamically less favorable as substrate binds, and we propose that it is the slowing down of this oxidation step at higher concentrations of substrate that is the origin of the inhibition. In contrast, we show that regeneration of the ferrous enzyme (and formation of NFK) in the final step of the mechanism, which formally requires reduction of the heme, is facilitated by the higher reduction potential in the substrate-bound enzyme and the two constants (k_{cat} and E_m^0) are shown also to be correlated. Thus, the overall catalytic activity is balanced between the equal and opposite dependencies of the initial and final steps of the mechanism on the heme reduction potential. This tuning of the reduction potential provides a simple mechanism for regulation of the reactivity, which may be used more widely across this family of enzymes.

INTRODUCTION

Indoleamine 2,3-dioxygenase (IDO) catalyzes the first and rate-limiting step in the kynurenine pathway, the O_2-dependent oxidation of L-tryptophan (L-Trp) to *N*-formylkynurenine, through cleavage of the C_2-C_3 bond of the substrate, Scheme 1. The mechanism of action of this dioxygenase activity is of increasing interest from a clinical perspective because tryptophan catabolism generates a number of secondary metabolites that are implicated in a wide range of neurological disorders, cataract formation, and suppression of T cell proliferation.[1] This extends to an understanding of enzyme inhibition, because the development of dioxygenase inhibitors is ongoing,[2] with some compounds in clinical trials.[3]

Scheme 1. Reaction Catalyzed by IDO

Tryptophan → (O2) → N-formylkynurenine

It was noted 40 years ago that the rate of tryptophan turnover in rabbit indoleamine 2,3-dioxygenase decreases at higher concentrations of substrate.[4,5] There have been several proposals for the origin of the inhibition by L-Trp, but a consensus has not been reached. It was originally assumed[4] to be a result of binding L-Trp to the ferric form of the enzyme. However, there are two difficulties with this interpretation. First, we have reported[6] for human IDO (hIDO) that binding of L-Trp to the ferric enzyme leads to an increase in reduction potential of the heme group; as we have noted previously,[7] early data reported similar observations in rabbit IDO.[8,9] Such an increase in reduction potential would actually stabilize formation of the catalytically

Received: September 15, 2011
Published: February 2, 2012

   dx.doi.org/10.1021/ja208694g | J. Am. Chem.Soc. 2012, 134, 3034−3041

active ferrous heme and thus would not, in isolation, be expected to lead to inhibition. Second, unlike other catalytic heme enzymes which require continuous recycling of the oxidized ferryl heme, the evidence so far indicates that only a single reduction of the ferric heme is required in IDO, after which the reaction needs no further reducing equivalents to proceed. Because of this, the binding of L-Trp to ferric heme would not be expected to inhibit turnover because ferric heme is not implicated catalytically.

In this contribution, we put forward an alternative hypothesis. We show that the overall enzyme activity, and hence the extent of the inhibition, is correlated with the heme reduction potential. This provides a simple mechanism for regulation of enzyme activity.

MATERIALS AND METHODS

Mutants of hIDO (S167H, S167A, F164A, F163A, F226A, F227A, F226Y, R231K) were prepared using the QuickchangeTM Site-directed Mutagenesis kit (Stratagene Ltd., Cambridge, UK). All variants were sequenced to confirm that no spurious mutations had occurred during the PCR and were expressed and purified according to previously published procedures. Human IDO (hIDO) and all site-directed variants were purified according to previously described procedures.[10] The variants fall into the following three main categories: (i) those in which a potential hydrogen-bonding residue is removed (Ser167 variants); (ii) those which affect the hydrophobic nature of the heme pocket (Phe variants); and (iii) those which affect hydrogen bonding to L-Trp[11] (Arg231 variant). His-tagged proteins were loaded onto a Ni-affinity column in 50 mM potassium phosphate buffer, pH 8, containing 0.3 M KCl, washed with the same buffer at pH 6, and then eluted with 0.25 M EDTA, pH 8. Eluted protein was loaded onto a Superdex 75 column (GE Healthcare) equilibrated with 0.1 M Tris HCl buffer, pH 8.3, containing 0.3 M KCl. Eluted fractions of pure protein had Soret peak at 404 nm. All kinetic experiments were carried out in 0.1 M Tris HCl buffer, pH 8, at 20.0 °C. Steady-state assays were carried out using methylene blue, ascorbate and catalase for reduction of heme as described previously[10] using a Perkin-Elmer Lambda 25 spectrophotometer. NFK formation was monitored at 321 nm and values of k_{cat} were extracted from initial rates (ΔAbs/min) by dividing by the absorption coefficient for NFK (ε_{321} = 3.75 mM^{-1} cm^{-1}) and the enzyme concentration. Reduction potentials were determined by the reduction of a dye with a known potential, according to published procedures.[10] Typically, the assay solution contained potassium phosphate buffer (0.1 M, pH 7.0), glucose (5 mM), xanthine (300 μM), xanthine oxidase (50 nM), glucose oxidase (50 μg/mL), catalase (5 μg/mL), enzyme (2 μM), and the appropriate dye. Spectral changes were monitored using a Perkin-Elmer Lambda 25 spectrophotometer (the components glucose, glucose oxidase, and catalase being used to generate an oxygen-free environment). Heme reduction potentials were determined by fitting the data to a Nernst equation for a single-electron process. All potentials are stated versus the normal hydrogen electrode (NHE). The dyes, all supplied by Sigma-Aldrich, were: phenosafranine (E^0_m = −252 mV), nile blue (−116 mV), methylene blue (+11 mV), toluidine blue (+34 mV).[12] Stopped-flow experiments were carried out using an Applied Photophysics SX.18MV stopped-flow spectrometer housed in an anaerobic glovebox (Belle Technology Ltd., [O_2] < 5 ppm) and fitted with a Neslab RTE-200 circulating water bath (±0.1 °C). Reactions were monitored in single wavelength mode (416, 576 nm) or using diode array. Reported values of k_{obs} were an average of at least four measurements, and all reactions were carried out under pseudo-first-order conditions. Data were collected over a period of 1 s from the mixing event, and traces were fitted to a single exponential process to give k_{obs} measured at different O_2 concentrations. For O_2 binding experiments, reactions were initiated by mixing anaerobic solutions of enzyme (typically 2 μM, degassed with N_2 and prereduced with dithionite) with an equal volume of fully degassed buffer containing O_2 at different concentrations (0.05–0.6 mM, prepared by mixing with a fully O_2-saturated solution of the same buffer). Equilibrium binding constants, K_d, for binding of L-Trp to ferrous enzyme (prepared by stoichiometric reduction with dithionite) were determined anaerobically in the presence of glucose (5 mM), glucose oxidase (50 μg/mL), and catalase (5 μg/mL).

RESULTS

Methodological Approach. The rate of catalytic turnover of IDO decreases at higher concentrations of L-Trp.[4,5] This has been observed for rabbit IDO[4] and more recently for hIDO.[13,14] In this analysis, we have interpreted the behavior according to Scheme 2. In this general mechanism, it is proposed that O_2 binds first (k_1), which through oxidation of the heme leads to the equivalent resonance form of ferric superoxide (Fe^{3+}–$O_2^{\bullet-}$). There is evidence for the presence of a ferric superoxide species from recent resonance Raman work,[15] which is consistent with the same formulation of this ferrous-oxy bond in the globins (see for example ref 16). This is followed by binding of L-Trp (k_3), leading to the formation of the ternary complex (Fe^{3+}–$O_2^{\bullet-}$–Trp), which subsequently converts to product with the rate constant k_{cat}. Scheme 2 dictates that under conditions where the concentration of L-Trp is very high (e.g., for enzyme inhibition), L-Trp will bind to the protein (k_2) before O_2 (k_4), such that the same ternary complex forms product and the resting enzyme is recovered (with the same rate constant, k_{cat}).

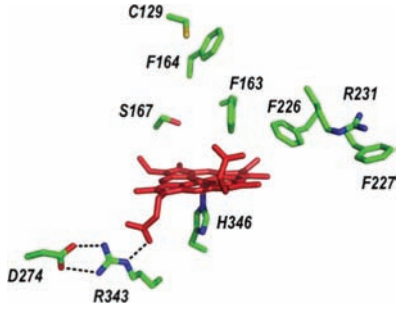

Figure 1. Active-site structure in hIDO, showing the locations of the residues targeted by mutagenesis in this work.[29]

We first analyze inhibition data obtained in this work according to Scheme 2, to extract the relevant inhibition constants. We go on to show that these inhibition constants depend on both k_1 and k_{cat}, and that k_1 and k_{cat} themselves are oppositely correlated with the reduction potential of the heme group. We probe these effects further with a number of mutants, Figure 1, which were selected with the aim of probing active-site structure and varying the heme reduction potential. We use this

Scheme 2. Mechanistic Scheme Used for Analysis of Substrate Inhibition

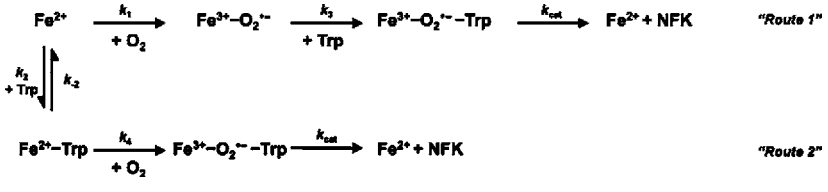

dx.doi.org/10.1021/ja208694g | J. Am. Chem.Soc. 2012, 134, 3034–3041

approach to present a hypothesis for substrate inhibition that is regulated by the reduction potential in wild-type hIDO and numerous site-directed variants.

Substrate Inhibition. Derivation of Relevant Equations. The rate of catalytic turnover of hIDO decreases at higher concentrations of L-Trp, as shown in Figure 2 for hIDO. The

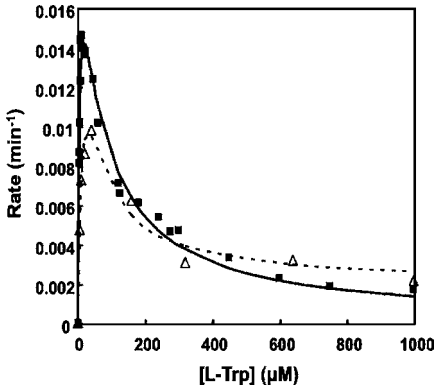

Figure 2. Plots of rate (ΔAbs min^{-1}) versus substrate concentration for hIDO (■) and the S167A variant of hIDO (△). Lines show fits of the data to eq 1; steady-state parameters extracted from the fit are listed in Table 1. Conditions: 0.1 M Tris-HCl, pH 8.0, [enzyme] = 100 nM, 30 μg/mL catalase, [ascorbate] = 20 mM, [methylene blue] = 10 μM, [O_2] = 258 μM, 20.0 °C.

derivations from the initial steady-state approximation are presented in the Supporting Information (derivation 1), giving rise to the following expression for the rate of the reaction, eq 1 (which is Eqn S8 in the Supporting Information):

$$\frac{d[NFK]}{dt} = \left(1 + \frac{[Trp]}{K_i^{eff,1}}\right)\frac{k_{cat}[hIDO][Trp]}{K_M + [Trp]\left(1 + \frac{[Trp]}{K_i^{eff}}\right)} \quad (1)$$

As we explain in the Supporting Information and again below, this expression is useful because it accommodates different kinds of inhibition.

If $k_{cat} \ll k_1[O_2]$, which is expected to be the case because k_{cat} is typically <20 s^{-1} for dioxygenases in general (and only ~1 s^{-1} for hIDO), and because k_1 is ~10^6 M^{-1} s^{-1}[10], then the Michaelis constant, K_M, is defined as in eq 2.

$$K_M = \frac{k_{cat}}{k_3} \quad (2)$$

In eq 1, there are two effective substrate inhibition constants, K_i^{eff} and $K_i^{eff,1}$. These constants have complicated expressions (see Supporting Information); however, they can be approximated by eqs 3 and 4 to correctly account for the limiting cases of strong and weak inhibition, so that,

$$K_i^{eff} \approx \frac{K_d k_1[O_2]}{k_{cat}} \quad (3)$$

where K_d is the binding constant of L-Trp to ferrous hIDO (Scheme 2, $K_d = k_{-2}/k_2$), and

$$K_i^{eff,1} \approx \frac{K_i^{eff} k_{cat}}{\tilde{k}_4} \quad (4)$$

where $\tilde{k}_4$ is defined as the overall (observed) rate of product formation (from the consecutive reactions) if L-Trp binds first (depicted as "route 2" in Scheme 2)

$$\tilde{k}_4 = \frac{k_{cat}[O_2]k_4}{k_{cat} + k_4[O_2]} \quad (5)$$

For eq 1 there are three types of behavior, each of which we have observed in our experiments and which can be rationalized with different ratios of K_i^{eff} and $K_i^{eff,1}$, see also Supporting Information (SI) (Derivation 1). Type 1 behavior shows *full inhibition* of the steady-state rate, as observed for hIDO (Figure 2) and F227A (Table 1), with the effective inhibition constant K_i^{eff}

Table 1. Summary of Reduction Potentials and Steady-State and Presteady-State Constants for hIDO and Site-Directed Variants[a]

protein	E^0_m (Fe^{2+}/Fe^{3+}) (mV)[f]	k_{cat} (s^{-1})	K_M (μM)	K_i^{eff} (μM)[d]	K_d (μM)[g]	$K_i^{eff}{}_{(calc)}$ (μM)[h]	$K_i^{eff,1}$ (μM)	k_1 (μM^{-1} s^{-1})[i,k]
hIDO[b]	−60	1.4 ± 0.1	5.0 ± 0.3	65 ± 6	0.7 ± 0.2	68	–	0.53 ± 0.03[j]
S167A[c]	−12	1.6 ± 0.1	22 ± 2	31 ± 2	0.7 ± 0.2	29	400 ± 100	0.25 ± 0.01
S167H	−200	0.0060 ± 0.0003	26 ± 3	–	–	10000	–	–
F163A[c]	−119	0.040 ± 0.002	68 ± 6	1700 ± 100	0.4 ± 0.1	2700	>10000	0.78 ± 0.04
F164A[c]	−85	0.68 ± 0.03	160 ± 10	400 ± 20	–	–	1300 ± 200	–
F226A[e]	−127	0.12 ± 0.01	310 ± 20	1000 ± 50	0.4 ± 0.1	750	970 ± 100	1.00 ± 0.05
F226Y[c]	18	6.0 ± 0.3	160 ± 10	10 ± 1	0.7 ± 0.2	5.0	98 ± 10	0.17 ± 0.01
F227A[b]	−116	0.40 ± 0.02	15 ± 2	–	0.2 ± 0.1	93	–	0.76 ± 0.04
R231K[e]	−106	0.30 ± 0.01	–	–	0.2 ± 0.1	410	–	0.70 ± 0.03

[a]The reduction potential for hIDO was previously published.[10]. [b]For this type of inhibition the rate goes to zero (Type 1, full inhibition), and $K_i^{eff,1}$ is out of experimental range (i.e., >10,000 μM); see eqn S8 in SI. [c]For this type of inhibition, K_i^{eff} and $K_i^{eff,1}$ are comparable (eq 1), and partial inhibition is observed (Type 3). [d]In some proteins, it was not possible to obtain reliable sets of inhibition data either because the enzyme was not stable enough under conditions of high concentration of tryptophan (for R231K and F227A) or because the steady-state activity is very low to begin with (for S167H). This means that values for inhibition constants (K_i^{eff}) could not be obtained (see Figure 5). [e]For this variant no inhibition is observed (Type 2). Both K_i^{eff} and $K_i^{eff,1}$ are large and out of experimental range. Normal Michaelis–Menten kinetics are therefore observed. [f]For reduction potentials, estimated errors of ±2 mV apply in all cases, which is largely a consequence of the uncertainty of the measured (literature) potential of the reference dye. [g]In some cases, it was not possible to determine a value for K_d because the absorbance changes were too small (for K_d). [h]Calculated using eq 3. [i]All second-order rate constants for O_2 binding, k_1, were determined experimentally by stopped flow (from a linear dependence of k_{obs} on [O_2]), except for the value presented for hIDO which has been reported previously.[10] [j]The second-order rate constant in the presence of L-Trp was observed to be lower (k_4 = 0.16 ± 0.02 μM^{-1} s^{-1}). [k]In some cases, it was not possible to determine a reliable value for k_1 because the ferrous oxy species was either unstable (F164A, S167H) or found not to be formed in 100% yields (S167H).

dx.doi.org/10.1021/ja208694g | J. Am. Chem.Soc. 2012, 134, 3034–3041

under conditions where the experimental concentration of L-Trp can exceed the magnitude of K_i^{eff}. In this case, K_i^{eff} is within experimental range, k_{cat} approaches zero at the limiting concentration of L-Trp, and $K_i^{eff,1}$ is (infinitely) large and is not experimentally accessible. Type 2 behavior occurs when K_i^{eff} itself is not experimentally accessible (i.e. $K_i^{eff} \gg$ [L-Trp]). In this case, *no inhibition* is observed, and k_{cat} does not decrease with increasing concentration of substrate, an example being the F226A variant, Figure S1(SI). Type 3 behavior is when k_{cat} reduces in value but does not approach zero, for example for the F226Y variant, Figure S1(SI), the S167A variant (Figure 2), and the F163A, F164A variants, Table 1. In this case, the additional constant $K_i^{eff,1}$ (which can be considered as the concentration of L-Trp at which the rate of product formation through routes 1 and 2 in Scheme 2 becomes equal, see derivation 2 in SI) is within experimental range (i.e., not infinitely large as above) but takes into consideration our observations for certain variants that the reaction may not always approach zero at high concentrations of L-Trp. In these cases *partial inhibition* is seen, because turnover is slowed down but can still proceed at a measurable rate even when L-Trp binds first (route 2 in Scheme 2, where $k_4 \neq 0$). One can see from eqs 1, 3, and 4 that *in extremis*, when the concentration of L-Trp is larger than either that of K_i^{eff} or $K_i^{eff,1}$, then the reaction rate is $\tilde{k}_4$ [hIDO] and that under these conditions of high tryptophan concentration, from eq 5 one can see that $\tilde{k}_4$ is small and approximates to $k_4[O_2]$ when $k_{cat} > k_4[O_2]$. The latter condition dictates that with binding of O_2 to the Fe^{2+}–Trp complex, k_4 must be slowed down in the presence of the substrate, which is the ultimate reason for the inhibition.

Data Analysis. Figure 2 shows the results of the substrate inhibition experiments for hIDO and an analysis of the experimental data according to Scheme 2 and fitted to eq 1. Best-fit values for the parameters k_{cat}, K_M, K_i^{eff}, and $K_i^{eff,1}$ are shown in Table 1 along with the reduction potential for hIDO (previously reported[10]). The corresponding fitted values for a number of site-directed variants are also presented in Table 1.

The validity of the fitting process can be verified because the extracted values for K_i^{eff} can be calculated independently from other experimentally accessible constants, as K_i^{eff} is itself the product of two terms, eq 3. The first, K_d, is the binding constant of L-Trp to ferrous hIDO ($K_d = k_{-2}/k_2$, Scheme 2), which was determined by anaerobic titration of reduced enzyme with L-Trp, Table 1. The second comes from the ratio $k_1[O_2]/k_{cat}$, where $[O_2]$ is constant (258 μM). Where reliable experimental values are available for k_1, values for K_i^{eff} can thus be calculated independently from K_d, k_1 and k_{cat} (eq 3) and compared with the experimental values. For instance for hIDO, k_{cat} = 1.35 s^{-1} (Table 1), k_1 = 0.53 μM^{-1} s^{-1},[10] and K_d = 0.7 μM, which yields K_i^{eff} = 68 μM. This is close to the value derived experimentally (K_i^{eff} = 65 μM, Table 1). Other calculated values for K_i^{eff} are shown in Table 1, and are likewise in good agreement with the experimental data. In general, less active hIDO variants have smaller values of k_{cat} which lead to larger values for K_i^{eff} according to eq 3, which accounts for the fact that substrate inhibition is not observed with these mutants (Type 2 behavior): F163A is an example, as K_i^{eff} is in the millimolar range and therefore inaccessible experimentally. Overall, these analyses show that reliable values for K_i^{eff} can be extracted (in the range of 5 μM to 2 mM) and that the experimental values are in reasonable agreement with calculated values.

Dependence of k_1 on Reduction Potential. We have reported[10] the reduction potential ($E^0{}_m$ (Fe^{3+}/Fe^{2+}) of hIDO as −63 mV (substantially lower than typically observed in the globins[17,18]) and that binding of L-Trp to hIDO increases the reduction potential to +18 mV in the presence of the substrate. In that work,[10] we made the preliminary observation that second-order rate constants for binding of O_2 to ferrous hIDO are affected by changes in the reduction potential of the heme group introduced by mutation. In particular, the S167A variant ($E^0{}_m$ (Fe^{3+}/Fe^{2+}) = −12 mV, which is 50 mV higher than hIDO), has a second-order rate constant for O_2 binding (k_1 = 0.25 $\mu M^{-1}s^{-1}$) that is 2-fold slower than that observed for hIDO (k_1 = 0.53 μM^{-1} s^{-1}), and the correlation between the rate constants is according to the expected dependence of the rate constant for Fe^{2+} oxidation on the reduction potential (because the oxy ferrous intermediate converts by oxidation to ferric superoxide), eq 6.

$$Fe^{2+} + O_2 \rightarrow Fe^{3+}-O_2^{\bullet -} \quad (6)$$

The following expression applies,

$$\ln k_1 = \text{const} - \alpha E^0{}_m(Fe^{3+}/Fe^{2+})/RT \quad (7)$$

where $0 < \alpha < 1$ is the Marcus transfer coefficient,[19] and $RT(= RT/F)$ = 25 mV at T = 20 °C.[a] As we show in the SI (derivation 2, Eqn SC), a linear expression can be derived by equating the two expressions for the wild type and variants. We present data for hIDO and a number of variants plotted in this way according to Eqn SC, Figure 3. The reduction potentials

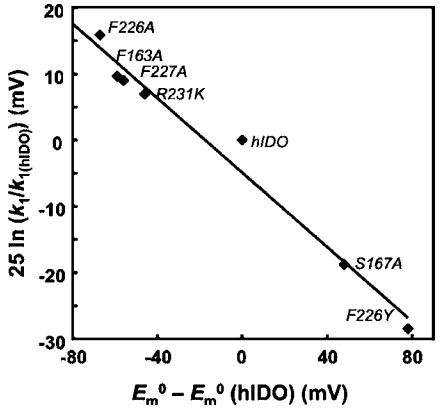

Figure 3. Logarithmic dependence of k_1 (see values given in Table 1), normalized to $k_{1\ (hIDO)}$, on the difference of the reduction potentials between the corresponding variant $E_m{}^0$ (Fe^{3+}/Fe^{2+}) and hIDO ($E_m{}^0$ (Fe^{3+}/Fe^{2+} (hIDO)). The F164A variant is not included in this plot because the stability of its ferrous oxy was too low to allow a meaningful determination of k_1 (see also data in Table 1).

used in these analyses are presented in Table 1, with a representative data set shown for the F226Y variant in Figure S2 (SI); second-order rate constants for O_2 binding, k_1, are also reported in Table 1, with representative data sets shown for the F227Y variant in Figure S3 (SI). A linear correlation of ln k_1 against reduction potential is observed across the range of variants, Figure 3, although there is some scattering of points. The average slope is calculated as α = 0.28, which is consistent with the analysis and discussed further below. To our knowledge, this dependence of the rate constant for O_2 binding with reduction potential appears to have been overlooked in previous studies.

Applying the same rate constant/reduction potential correlation, according to Scheme 2, one can predict that when L-Trp binds first the positive shift in potential (81 mV for hIDO[10])

dx.doi.org/10.1021/ja208694g | J. Am. Chem.Soc. 2012, 134, 3034−3041

should decelerate the subsequent binding of O_2 to the hIDO–Trp complex (k_4) according to eq 7, because the formation of ferric-superoxide heme from oxidation of ferrous oxy heme is redox driven and can be analyzed as such. Accordingly, when the Fe^{3+}/Fe^{2+} potential is increased, the rate constant k_4 is expected to decrease, and one can predict that it slows down by $\exp(-\alpha((E^0_m(Fe^{3+}/Fe^{2+}) - E^0_m(Fe^{3+}\text{–Trp}/Fe^{2+}\text{–Trp}))/RT) = \exp(0.24 \times 81/25) = 2.1$ times. This conclusion is verified by stopped-flow experiments in which formation of Fe^{II}–O_2 (monitored at 570 nm) was faster in the absence of tryptophan ($k_1 = 0.53 \pm 0.06\ \mu M^{-1}\ s^{-1}$) than after preincubation of ferrous hIDO with L-Trp ($k_4 = 0.16 \pm 0.02\ \mu M^{-1}\ s^{-1}$, Table 1). The experimentally determined ratio $k_1/k_4 = 3.3$ is in good agreement with the predicted value of 2.1 calculated from the shift in the reduction potentials.

Dependence of k_{cat} on Reduction Potential. In the preceding section we have shown that the kinetics of O_2 binding to ferrous hIDO were correlated with the reduction potential of the heme iron, Figure 3, as described by eq 7. One can further expand this approach and also consider the rate-determining final step (k_{cat}) in Scheme 2 as a redox process because it involves formal "re-reduction" of the heme, eq 8.[b]

$$Fe^{3+}\text{–}O_2^- - Trp \rightarrow Fe^{2+} + [O_2\text{–}Trp] \quad (8)$$

When considering this as an electrochemical process, a similar expression for the rate constant can be proposed, eq 9.

$$\ln k_{cat} = \text{const} + (1 - \alpha)E^0_m(Fe^{3+}/Fe^{2+})/RT \quad (9)$$

This shows that the dependence of k_{cat} on reduction potential is also exponential (as it is for k_1 in eq 7), but there is an important difference: the transfer coefficient must be $1 - \alpha$, since it is the reverse reaction that is being considered. Experimental verification of this requirement imposes a crucial check on the validity of the model.

The experimental data for hIDO and a number of variants are shown in Figure 4, where plots of ln k_{cat} for each variant (using a derivation similar to k_1 above, see Supporting Information, Eqn (SD)) are shown as a function of the corresponding difference in the reduction potential between hIDO and the variant (Table 1). The dependence fits a linear function according to eq 9. Moreover, the transfer coefficient (from the slope) is $1 - \alpha = 0.76$ according to eq 9. This means that $\alpha = 0.24$ which is in very good agreement with the estimate of $\alpha = 0.28$ from the O_2-binding experiment shown in Figure 3 (above), providing a reliable test of the methodology.

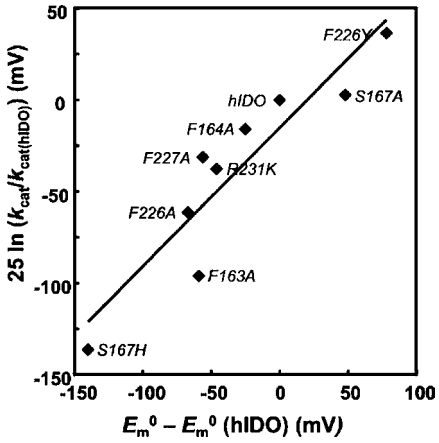

Figure 4. Logarithmic dependence of k_{cat}, normalized to $k_{cat\ (hIDO)}$, on the difference of the reduction potentials between the corresponding variant E_m^0 (Fe^{3+}/Fe^{2+}) and hIDO E_m^0 (Fe^{3+}/Fe^{2+} (hIDO)). See also data in Table 1 (and footnote k).

Overall Dependence of Enzyme Inhibition (K_i^{eff}) on Reduction Potential. The above analyses for k_1 and k_{cat} show that they are oppositely correlated with the heme reduction potential, Figures 3 and 4. But both of these terms contribute to the inhibition constant, K_i^{eff}, extracted from Figure 2, because $K_i^{eff} = K_d k_1[O_2]/k_{cat}$, eq 3). From eq 7 for k_1 and eq 9 for k_{cat}, one sees that the transfer α coefficient cancels, since $k_1/k_{cat} \approx \exp(-\alpha E^0_m(Fe^{3+}/Fe^{2+})/RT)/\exp((1 - \alpha)E^0_m(Fe^{3+}/Fe^{2+})/RT) = \exp(-E^0_m(Fe^{3+}/Fe^{2+})/RT)$.

Combining the pre-exponential factors into a single potential independent constant, one derives eq 10:

$$\ln K_i^{eff} = \text{const} - \frac{E^0_m(Fe^{3+}/Fe^{2+})}{RT} \quad (10)$$

which gives an expression for the *overall* dependence of K_i^{eff} on the reduction potential, which is contributed by the equal and opposite effects of the dependence of k_1 and k_{cat} on the reduction potential. As above for k_1, a linear expression can be derived by equating the two expressions for the wild type and variants (derivation 2 in SI, Eqn SE). Accordingly, a logarithmic plot of Eqn SE, Figure 5, is expected to be linear. The data show that this is indeed the case, and the slope (= 0.86 ± 0.05) is close to unity which means that the assumptions leading to eq 10 are correct.[c]

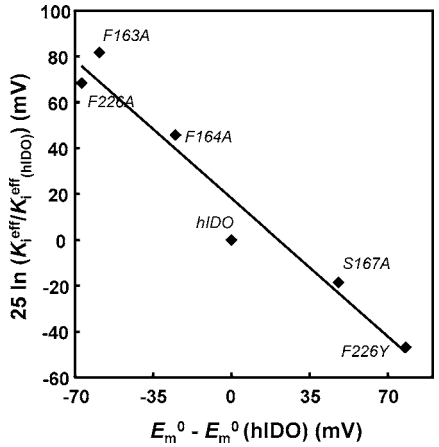

Figure 5. Logarithmic plot of the dependence of K_i^{eff} (Table 1), normalized to $K_i^{eff}{}_{(hIDO)}$, on the difference of the reduction potentials between the corresponding variant E_m^0 (Fe^{3+}/Fe^{2+}) and hIDO E_m^0 (Fe^{3+}/Fe^{2+} (hIDO)). See also data in Table 1 (and footnote d).

DISCUSSION

Substrate inhibition of IDO has long been a feature of the literature,[5,20] but the mechanism of inhibition has not been established. It has been suggested[4] to originate from the unproductive binding of L-Trp to the catalytically inactive ferric form of the enzyme. However, in 2005 we noted[6] that the reduction potential for human IDO (hIDO) increases on binding of L-Trp, and this is not consistent with such an interpretation.

Origin of the Inhibition. Recently, it has been proposed from steady-state analyses[13] that a second binding site for L-Trp is the source of the inhibition in hIDO. There may indeed be a second (weak) binding site,[13,14,21] and at high enough concentrations

dx.doi.org/10.1021/ja208694g | J. Am. Chem.Soc. 2012, 134, 3034–3041

the substrate may well bind at more than one location or in multiple conformations[22] within the distal cavity (although spectroscopic data suggest that multiple conformations of substrate orientation are not likely in the presence of O_2[23]). We do not exclude the possibility of a second site at high concentrations of Trp, most likely above those found physiologically, but we can account for the inhibition without needing to invoke binding at a second, inhibitory site (physiological concentrations of tryptophan are not well documented but are probably in the range 40−100 μM[24,25]). Indeed, the crystal structure of hIDO shows two CHES molecules in the active site, which might be an indication of a larger, more open active site. However, a fit of kinetic inhibition data to this kind of dependence does not, *ipso facto*, establish the existence of a second site. We find that substrate inhibition in hIDO can be rationalized by assuming only a single binding site for L-Trp for the wild-type protein and all variants. We do not exclude the possibility of a second site at high concentrations of Trp (most likely above those found physiologically), but we can account for the inhibition without needing to invoke binding at a second, inhibitory site. Our analyses go beyond just the fitting of steady-state inhibition data and include an examination of the effect of reduction potential on both O_2 binding (k_1) and turnover (k_{cat}). We have demonstrated that the inhibition constant is correlated first with k_1, Figure 3, and oppositely with oppositely with k_{cat}, Figure 4 (as well as with K_d) and that the reduction potential dependence of the inhibition constant is exactly correlated with the expected reduction potential dependence of both k_1 and k_{cat} across a range of variants. There are essentially three types of inhibition behavior, Scheme 2.

(i) In the case of normal substrate inhibition (e.g., for the wild-type protein and also F227A, Type 1) O_2 binds first followed by binding of L-Trp. This means that at low substrate concentrations the rate of the first step (formation of ferric superoxide (= $k_1[Fe^{2+}][O_2]$)) is fast and product formation occurs through "route 1" of Scheme 2; under conditions of high L-Trp concentrations, L-Trp binding out-competes O_2 binding, but then formation of the ternary complex (= $k_4[Fe^{2+}{-}Trp][O_2]$) becomes rate limiting and, *in extremis*, approaches zero (Type 1 inhibition).

(ii) In the case where no substrate inhibition is observed (Type 2, e.g. for F226A and R231K), either O_2 (k_1) or Trp (k_2) can bind first, but binding of Trp ("route 2" in Scheme 2) does not block activity at all, so that no inhibition is observed ($k_1 \approx k_4$).

(iii) In cases where partial inhibition (Type 3) is observed (e.g., S167A, F163A, F164A, and F226Y), binding of substrate at high concentrations reduces but does not completely block activity, so that the reaction can still proceed by both routes productively and slows down at high concentrations of substrate but not to zero ($k_1 > k_4$, and $k_4 \neq 0$).

This analysis can account for the long-documented[4,5] lack of inhibition (reproduced recently[13]) seen for IDO against D-Trp, because if K_d for D-Trp binding in IDO is larger than for L-Trp (as it is, for example, in human TDO[7]) then K_i^{eff} is correspondingly large (eq 3) and out of range, and no inhibition is expected. The analysis also accounts for the fact that hTDO does not show substrate inhibition at all.[7,26] Rather than exhibiting preferential binding of substrate to the reduced enzyme (as observed by us[6] and others[14] in hIDO), binding of L-Trp to ferrous hTDO is much weaker[7,26] which again may be understood in terms of our proposed model, because increases in K_d will correspondingly increase K_i^{eff}, so that substrate inhibition is not observed.

A Quantitative Correlation of Older Data. The analysis also helps to clarify several older reports in the published literature. A qualitative correlation between activity and the electron-withdrawing capacity (which can be considered as correlated with the reduction potential) of heme had been noted previously, but its implications had not been quantified or widely appreciated. It was shown some years ago[27] that the logarithm of the turnover rate is linearly correlated with reduction potential in TDO reconstituted with variously substituted heme prosthetic groups (which have different reduction potentials). But the experiments were carried out on different enzymes, which meant that the observations were correlated only qualitatively, with the authors simply noting that "the catalytic activity of L-tryptophan 2,3-dioxygenase increases as the affinity of the enzyme for oxygen increases". This is precisely the behavior that we describe, and so we have used our eqs 7 and 9 to quantify the previously published data.[27] If we take the previously published values[27] for k_{cat} (for TDO) and the binding constant of the ferrous enzyme for O_2 and reanalyze the original data in the same way as we have done above for IDO, we observe the expected logarithmic dependence (with one rogue data point in each case, Figure 6). This analysis further supports our conclusions, and the two sets of experiments can in fact be regarded as similar—on the one hand by changing reduction potential by substitution of the heme group[27] and on the other by mutation (this work)—but giving the same overall correlation.

pH-Dependence of Substrate Inhibition. Our analyses also help to clarify other aspects of the older literature.[4] First, Sono and co-workers[4] have shown for rabbit IDO that substrate inhibition is stronger at higher pH (Figure 6 in ref 4) and separately that there is a decrease in K_d for L-Trp binding to ferrous IDO with increasing pH (Figure 5 in ref 4, which is the same dependence as that observed for hIDO[6]).

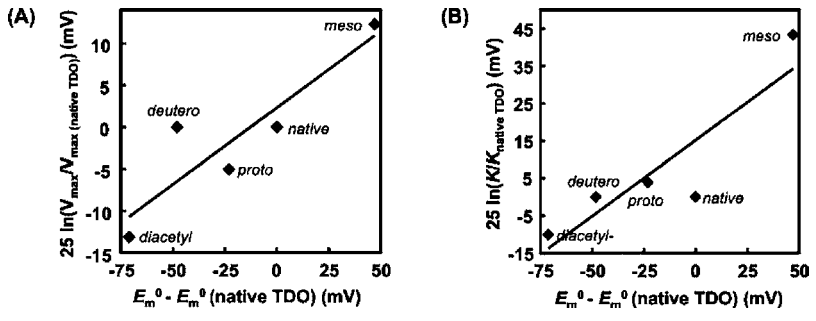

Figure 6. Plots of previously published[27] data (taken from Table 1 of ref 25) showing (A) ln V_{max} and (B) ln $K_{50(O2)}$ for heme-substituted TDO as a function of reduction potential of the corresponding heme. V_{max} is the maximal turnover rate, and $K_{50(O2)}$ is the O_2 affinity.

dx.doi.org/10.1021/ja208694g | J. Am. Chem.Soc. 2012, 134, 3034−3041

These observations are reconciled by eq 3, because the inhibition constant K_i^{eff} is proportional to K_d so that the observed[4] decrease in K_d at higher pH leads directly to a corresponding decrease in K_i^{eff}, thus accounting for the stronger inhibition.

Second, it was concluded[4] that inhibition was caused by binding of Trp to the ferric enzyme because the inhibition constant was found to be of a magnitude similar to that of the K_d for binding of L-Trp to *ferric* enzyme (i.e., in the millimolar range). This seems unlikely, because in fact K_i^{eff} (Table 1) is less than 100 μM, which is much lower than the binding constant for Trp binding to *ferric* enzyme (most recent determinations put the K_d for L-Trp binding to ferric enzyme as very much higher, in the millimolar range[6,13,14,28]). Our model resolves this problem, because it implicates K_d only for the *ferrous* enzyme. The inhibition constant, K_i^{eff}, is equal to K_d multiplied by the factor $k_1[O_2]/k_{cat}$, eq 3, which shifts the value of K_d for the ferrous enzyme to a much higher value (from the submicromolar range to much higher (tens of micromoles)), and therefore in close agreement with the values for K_i^{eff}. As we explained in the Introduction, there are other conceptual problems with the idea that binding of L-Trp to ferric enzyme is the source of the inhibition.

CONCLUDING REMARKS

There has been considerable confusion in the literature on the order of substrate binding in the dioxygenases. In hIDO at least, our data clearly indicate that O_2 binding precedes Trp binding because if this binding order is reversed the increase in reduction potential as a consequence of Trp binding disfavors the subsequent O_2 binding step. There is an informative analogy here with the P450s. In the P450s, substrate binding can also be accompanied by an increase in reduction potential of the heme, although in this case the substrate binds to ferric heme, and the increase in potential facilitates the subsequent reduction and turnover—a molecular 'gate' that needs to be 'opened' during every turnover cycle. In IDO, there is no need for continuous reduction of the heme because only a single (initiating) reduction is required. Consequently, the increase in reduction potential on substrate binding in IDO is not used in the same way; instead, the increase in reduction potential stabilizes the ferrous form and slows down O_2 binding. We propose that this is the source of the inhibition at high substrate concentrations, thus dictating that O_2 binds first.

ASSOCIATED CONTENT

Supporting Information

The derivation of relevant equations, steady-state data for variants (Figure S1) and representative reduction potential (Figure S2) and O_2 binding (Figure S3) data. Complete ref 11. This material is available free of charge via the Internet at http://pubs.acs.org.

AUTHOR INFORMATION

Corresponding Author

emma.raven@le.ac.uk

ACKNOWLEDGMENTS

This work was supported by grants from The Wellcome Trust (083636 to E.R. and to S.K.C./C.G.M.) and EPSRC (studentship to N.C.).

ADDITIONAL NOTES

[a]In all calculations for variants we assume that the "const" in eq 7) (and in eq 9) is not altered by the mutations, so that only the reduction potential is changed. To simplify formulas, we use RT instead of RT/F in all cases (which is equivalent, if it is measured in mV).

[b]In eq 8, the formation of the product NFK is shown schematically as $[O_2-Trp]$ to allow only the charge transfer processes to be easily visualized.

[c]The finding that $\alpha = 0.28$ is conserved for k_1 and k_{cat} (where it is $1 - \alpha$, with $\alpha = 0.24$) reflects the fact that both reactions have the same geometry of transition state, in which charge is redistributed between iron and oxygen.

REFERENCES

(1) Rohrig, U. F.; Awad, L.; Grosdidier, A.; Larrieu, P.; Stroobant, V.; Colau, D.; Cerundolo, V.; Simpson, A. J.; Vogel, P.; Van den Eynde, B. J.; Zoete, V.; Michielin, O. *J. Med. Chem.* **2010**, *53*, 1172−1189.

(2) Macchiarulo, A.; Camaioni, E.; Nuti, R.; Pellicciari, R. *Amino Acids* **2009**, *37*, 219−229.

(3) Katz, J. B.; Muller, A. J.; Prendergast, G. C. *Immunol Rev* **2008**, *222*, 206−221.

(4) Sono, M.; Taniguchi, T.; Watanabe, Y.; Hayaishi, O. *J. Biol. Chem.* **1980**, *255*, 1339−1345.

(5) Yamamoto, S.; Hayaishi, O. *J. Biol. Chem.* **1967**, *242*, 5260−5266.

(6) Papadopoulou, N. D.; Mewies, M.; McLean, K. J.; Seward, H. E.; Svistunenko, D. A.; Munro, A. W.; Raven, E. L. *Biochemistry* **2005**, *44*, 14318−14328.

(7) Basran, J.; Rafice, S. A.; Chauhan, N.; Efimov, I.; Cheesman, M. R.; Ghamsari, L.; Raven, E. L. *Biochemistry* **2008**, *47*, 4752−4760.

(8) Makino, R.; Sakaguchi, K.; Iizuka, T.; Ishimura, Y. *J. Biol. Chem.* **1980**, *255*, 11883−11891.

(9) *L-Tryptophan 2,3-dioxygenase; structure, function and interaction with substrate*; Makino, R.; Sakaguchi, K.; Iizuka, T.; Ishimura, Y., Eds. Amsterdam, 1980.

(10) Chauhan, N.; Basran, J.; Efimov, I.; Svistunenko, D. A.; Seward, H. E.; Moody, P. C. E.; Raven, E. L. *Biochemistry* **2008**, *47*, 4761−4769.

(11) Forouhar, F.; et al. *Proc. Natl. Acad. Sci. U.S.A.* **2007**, *104*, 473−478.

(12) Clark, W. M. *Oxidation-Reduction Potentials of Organic Systems*; Robert E. Kreiger Publishing Co.: Huntington, NY, 1972.

(13) Lu, C.; Lin, Y.; Yeh, S. R. *J. Am. Chem. Soc.* **2009**, *131*, 12866−12867.

(14) Lu, C.; Lin, Y.; Yeh, S. R. *Biochemistry* **2010**, *49*, 5028−5034.

(15) Lewis-Ballester, A.; Batabyal, D.; Egawa, T.; Lu, C.; Lin, Y.; Marti, M. A.; Capece, L.; Estrin, D. A.; Yeh, S. R. *Proc. Natl. Acad. Sci. U.S.A.* **2009**, *106*, 17371−17376.

(16) Chen, H.; Ikeda-Saito, M.; Shaik, S. *J. Am. Chem. Soc.* **2008**, *130*, 14778−14790.

(17) Lloyd, E.; King, B. C.; Hawkridge, F. M.; Mauk, A. G. *Inorg. Chem.* **1998**, *37*, 2888−2892.

(18) Raven, E. L.; Mauk, A. G. *Adv. Inorg. Chem.* **2001**, *51*, 1−49.

(19) Marcus, R. A. *Annu. Rev. Phys. Chem.* **1964**, *15*, 155−196.

(20) Shimizu, T.; Nomiyama, S.; Hirata, F.; Hayaishi, O. *J. Biol. Chem.* **1978**, *253*, 4700−4706.

(21) Nickel, E.; Nienhaus, K.; Lu, C.; Yeh, S. R.; Neinhaus, G. U. *J. Biol. Chem.* **2009**, *284*, 31548−31554.

(22) Capece, L.; Arrar, M.; Roitberg, A. E.; Yeh, S. R.; Marti, M. A.; Estrin, D. A. *Proteins* **2010**, *78*, 2961−2972.

(23) Davydov, R. M.; Chauhan, N.; Thackray, S. J.; Anderson, J. L.; Papadopoulou, N. D.; Mowat, C. G.; Chapman, S. K.; Raven, E. L.; Hoffman, B. M. *J. Am. Chem. Soc.* **2010**, *132*, 5494−5500.

(24) Cook, J. S.; Pogson, C. I. *Biochem. J.* **1983**, *214*, 511−516.

(25) Braidy, N.; Grant, R.; Brew, B. J.; Adams, S.; Jayasena, T.; Guillemin, G. J. *Int. J. Tryptophan Res.* **2009**, *2*, 61−69.

(26) Batabyal, D.; Yeh, S.-R. *J. Am. Chem. Soc.* **2009**, *131*, 3260−3270.
(27) Makino, R.; Iizuka, T.; Sakaguchi, K.; Ishimura, Y. *Oxygenases Oxygen Metab., Symp. Honor Osamu Hayaishi* **1982**, 467−477.
(28) Rosell, F. I.; Kuo, H. H.; Mauk, A. G. *J. Biol. Chem.* **2011**, in press.
(29) Sugimoto, H.; Oda, S.-i.; Otsuki, T.; Hino, T.; Yoshida, T.; Shiro, Y. *Proc. Natl. Acad. Sci. U.S.A.* **2006**, *103*, 2611−2616.